Journal of Computer Science

Research Article

Enhancing Kidney Stone Detection Accuracy Using Image Processing and a Hybrid Convolutional Deep Belief Network

Geetha M. N[1], Barkathulla A[2], S. Nandhini Devi[3], Garaga Srilakshmi[4], K. Swanthana[5], Jayaraj Ramasamy[6], Mohamed Uvaze Ahamed Ayoobkhan[7] and V. Bhoopathy[8]

[1]*Department of Electronics and Communication Engineering, Vidyavardhaka College of Engineering, Mysuru, Karnataka, India*
[2]*Department of Computer Science and Engineering, Vel Tech Rangarajan Dr. Sagunthala R&D Institute of Science and Technology, Avadi, Chennai, Tamil Nadu, India*
[3]*Department of Artificial Intelligence and Data science, V.S.B. Engineering college, Karur, TN, India*
[4]*Department of Electronics and Communication Engineering, Aditya University, Surampalem, Andhara Pradesh, India*
[5]*Department of Computer Science and Engineering, Koneru Lakshmaiah Education Foundation, Bowrampet, Hyderabad, Telangana, India*
[6]*Department of Computer Science, Coventry University, Kazakhstan*
[7]*School of Digital Technologies, American University of technology, Tashkent, Uzbekistan*
[8]*Department of Computer Science and Engineering, Sree Rama Engineering College, Tirupathi, India*

Article history
Received: 23-02-2025
Revised: 31-12-2025
Accepted: 02-01-2026

Corresponding Author:
V. Bhoopathy
Department of Computer Science and Engineering, SreeRama Engineering College, Tirupathi, India
Email: v.bhoopathy@gmail.com

Abstract: Automated CKD is a rapidly expanding non-communicable ailment that significantly contributes to global mortality and morbidity. CKD impacts more than 10% of the worldwide population, leading to millions of deaths annually. This paper proposes an enhanced deep learning model for renal disease detection that integrates convolutional and involution layers to enhance classification accuracy. CKD is a worldwide health issue characterised by the consequences of diminished renal function and renal failure. A KS is a condition that adversely affects renal function. The often asymptomatic nature of this illness necessitates fast and correct identification of renal problems to avert catastrophic consequences. This paper introduces an automated detection system for CT kidney stone images utilising a ConvDBN Model. The suggested study entails the preliminary augmentation of image phases, employing GB + LF, MB + LP, and Bilateral Filter to improve the quality of CT images of the kidneys. GLCM is utilised for feature extraction. Subsequently, ConvDBNs are utilised as a neural network approach for classification, primarily aimed at accurately differentiating between normal and abnormal photographs. Upon an aberrant classification suggesting the existence of a kidney stone, a subsequent measure is enacted. This phase entails the removal of the bed mat and the application of noise reduction techniques to achieve accurate detection and localisation of the kidney stone within the image. The suggested solution attains 98.2% accuracy utilising both quality and noisy image datasets, surpassing previous DL and conventional detection of image methods. To help urologists confirm their physical examination of KS, this automated method can be used to reduce the possibility of human error.

Keywords: Computed Tomography (CT), Chronic Kidney Disease (CKD), Gray Level Co-Occurrence Matrix (GLCM), Laplacian Filter (LF), Gaussian Blur (GB), Median Blur (MB), Convolutional Deep Belief Network (ConvDBN), Restricted Boltzmann Machine (RBM), Kidney Stone (KS), Picture Archiving and Communication System (PACS)

Introduction

All countries have a high prevalence of kidney illnesses, including nephrolithiasis, also known as kidney stones. In order to aid in early detection, treatment, and a reduction in the effects of nephrolithiasis, data mining is being used to try to establish a predictive model for identifying individuals and the type of stones (Kazemi and

SCIENCE Publications

© 2026 Geetha M. N, Barkathulla A, S. Nandhini Devi, Garaga Srilakshmi, K. Swanthana, Jayaraj Ramasamy, Mohamed Uvaze Ahamed Ayoobkhan and V. Bhoopathy. This open-access article is distributed under a Creative Commons Attribution (CC-BY) 4.0 license.

Mirroshandel, 2018). Characterising stones now necessitates meticulous manual measurement, complicating clinical decision-making and augmenting intra and inter-rater variability, hence hindering the analysis of numerous imaging data undertaken for therapeutic trials. These restrictions make it difficult to accurately determine the stone burden, which might result in less-than-ideal treatment plans and results, especially for doctors who don't examine the images themselves. Radiologists sometimes overlook other crucial clinical signs in kidney stones, such as the increased density of renal papillae, which is difficult to physically detect but is related to stone activity (Aksakalli et al., 2021). For instance, they only report the largest or most clinically conspicuous stones.

The lack of completely automated diagnostic imaging analyses that can precisely identify and quantify kidney stone features is a major barrier to improving the efficacy and efficiency of individualised care. The aim of this study was to evaluate the effectiveness of a constructed neural network system in autonomously recognising kidney stones and measuring key stone characteristics, including size, volume, location, and density (Kumar et al., 2024). Preventing kidney stones from forming and recurring is still a major concern for human health. Impairment of renal function resulting from the production of nephroliths jeopardises human life. Consequently, prompt identification of nephrolithiasis is essential. In recent years, technological advancements have led to the adoption of ML and DL methodologies for disease diagnosis (Busi et al., 2023). These methods offer a dependable instrument for rendering conclusive diagnostic determinations that necessitate lengthy and intricate procedures, since they reduce the duration of diagnosis and enhance diagnostic precision. In conjunction with deep learning, computer vision can classify images, extract their attributes, and facilitate image categorisation by making predictions based on the developed model. Numerous studies have been undertaken to identify diseases using deep learning approaches up to the present day.

Literature Survey

The utilisation of image processing techniques in medical imaging has transformed the analysis and interpretation of medical pictures. Segmentation, noise reduction, and feature extraction are prevalent tasks in image processing, as articulated by Asif et al. (2024). These approaches have been crucial in improving the visualisation of kidney stones in ultrasonographic pictures. The automation of kidney stone diagnosis with NN algorithms has garnered attention. Lopez-Tiro et al. (2024) demonstrated the effective application of deep learning for the identification and categorisation of kidney stones. These algorithms have demonstrated potential in optimising the diagnostic process and minimising subjectivity in stone characterisation. Rajan et al. (2023) indicated that a DCNN applied to 63 human kidney stones of diverse compositions in a prior pilot investigation could effectively predict kidney stone composition from digital photos. This study sought to examine the prediction of urolithiasis components with a DL algorithm utilising images of urinary stones acquired during endoscopic surgery (Ahmed et al., 2024). The application of NN addresses the challenges associated with the laborious and time-intensive task of precise stone detection and localisation. Ma et al. (2024) developed five distinct deep learning models for renal stone processing. Of the five models, the DL model utilising the XBOOST classifier yields superior results for accuracy, precision, and recall rates. Huang et al. (2023) proposed a radiomics algorithm for classifying kidney stones in non-contrast CT images. The suggested radiomics approach employs multivariable LR analysis for stone detection by extracting morphological and textural data. Ultimately, ensemble learning utilising bagged trees is employed for classification (Manjunatha et al., 2024). The results of the decision curve demonstrated that the proposed algorithm possesses greater efficacy in stone categorisation. Zhu et al. (2024) examined the efficacy of various classifiers, including DT, ANN, and Rule-based Classifiers, for stone categorisation. The proposed approach incorporates ensemble learning to enhance classification accuracy (Bayram et al., 2022). The allocation and modification of weights for each classifier is executed using a genetic algorithm. The classifier's total accuracy is elevated to 97.2% by appropriate weight modifications via the genetic algorithm. Nedbal et al. (2024) sought to classify patients based on the presence or absence of kidney stones utilising CT scans. The utilised dataset comprises CT scans from 433 patients. A unique categorisation network named ExDark19 was proposed in the study. The classification network was trained with the transfer learning approach. The kNN technique was employed as a classifier. A classification accuracy of 99.22% was attained. Pande and Agarwal (2024) sought to detect and fragment kidney stones utilising CT imaging. The utilised dataset comprises CT scans from 167 patients for segmentation tasks and 282 patients for classification tasks. A novel method named S.T.O.N.E was proposed for the classification problem in the study. The 3D U-Net segmentation network was employed in the segmentation task. A DSC of 97% was attained. This research proposes an enhanced CDBN model based on the preceding analysis (Zhang et al., 2024). A cross-entropy-based sparse penalty mechanism, appropriate for the CRBM model, is utilised to address the homogeneity issue of the CRBM unit. Additionally, drawing from the multi-layer supervised DBN model, a learning

DOI: 10.3844/jcssp.2026.3042.3052

methodology that alternates between supervised and unsupervised processes to train parameters is proposed to address the issue of gradient diffusion.

Proposed Methods

Kidney stone disease is a silent killer with a high morbidity rate; this is a major worry for healthcare systems worldwide. To lessen the impact of this disease and its expenses, advanced data mining methods like categorisation can aid in early disease prediction. In order to provide a decision-support system, the current work aims to derive a model for early diagnosis of the kind of kidney stone and the most significant characteristics. Because it could combine unsupervised pretraining (via Restricted Boltzmann Machines) with deep feature extraction (by convolutional layers), the ConvDBN (Convolutional Deep Belief Network) was selected over conventional deep models including CNN, ResNet, or U-Net. ConvDBNs use unsupervised learning to capture intricate data distributions, unlike CNNs, which are supervised and prone to overfitting in small datasets. Although strong, ResNet and U-Net are deeper architectures usually optimised for segmentation rather than classification and need greatly more data and processing resources. Using supervised-unsupervised training alternation and sparse penalty mechanisms, the hybrid ConvDBN also reduces vanishing gradients and improves generalisation.

The ConvDBN model proficiently identifies and localises kidney stones in CT images via a sequence of convolutional layers that autonomously extract pertinent characteristics, as shown in Fig. 1. These layers function as filters, incrementally extracting increasingly intricate information as the network deepens (Ramesh et al., 2023). The incorporation of ConvDBN enhances the training of deeper networks by alleviating the degradation issue faced in extremely deep architectures. Furthermore, the ConvDBN model aids in size and parameter identification, essential for precise diagnosis. By integrating the advantages of both designs, the model excels at identifying the nuanced differences characteristic of kidney stones. The model's learnt hierarchical characteristics allow it to adaptively recognise and characterise stones, hence enhancing detection precision. The hybrid ConvDBN model integrates deep belief networks for robust hierarchical learning with convolutional layers for feature extraction. Its main benefits consist of improved generalisation, and neurone over-activation is lowered via a sparse penalty mechanism. Supervised-unsupervised training alternately helps to reduce gradient vanishing. Better feature abstraction from CRBM layers; outperforms conventional CNNs, DBNs, or SVM-based hybrids. Even with CT images prone to noise generation, it achieves high detection accuracy 98.2%. This is especially valuable in medical diagnostics for jobs requiring interpretability, scalability, and precision.

Dataset

Using the PACS from multiple hospitals in Dhaka, Bangladesh (Kidney Disease Detection (Normal-Cyst-Tumor-Stone) n.d.), we assembled the CT kidney dataset. A number of Dhaka's hospitals provide care to a diverse range of metropolitan residents. The dataset likely includes individuals from a variety of socioeconomic backgrounds, improving its capacity to portray urban patients in Bangladesh, because Dhaka is a densely populated and culturally varied metropolis (Almuayqil et al., 2024). Images of patients with cysts, tumours, stones, or normal kidneys are all part of this dataset.

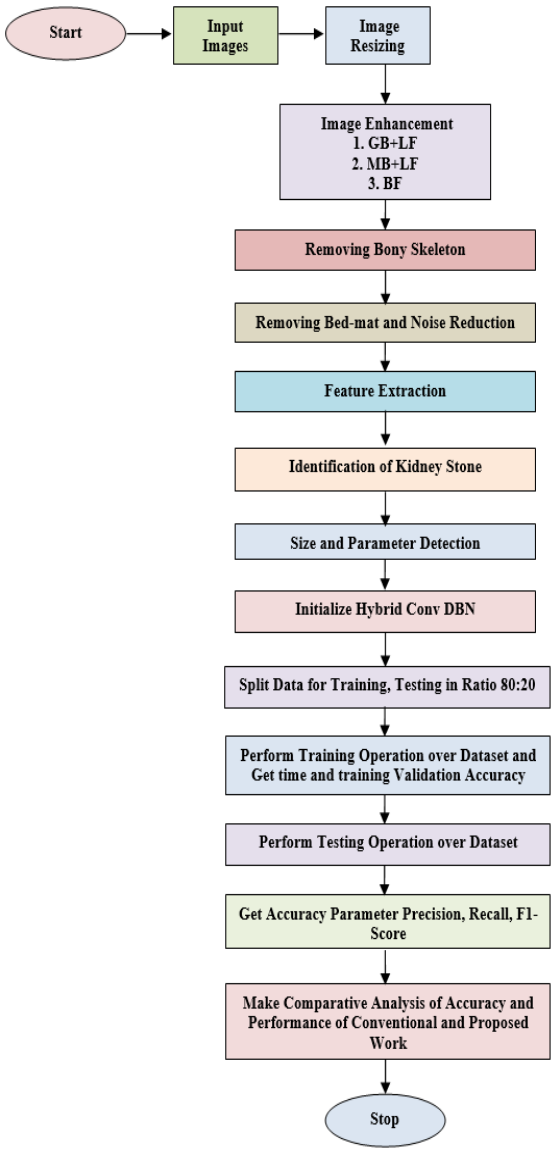

Fig. 1: Proposed process flow for detecting kidney stones

DOI: 10.3844/jcssp.2026.3042.3052

Table 1: Class distribution of kidney stone dataset

Class	Count of images
Cyst	3709
Stone	1377
Normal	5077
Tumor	2283

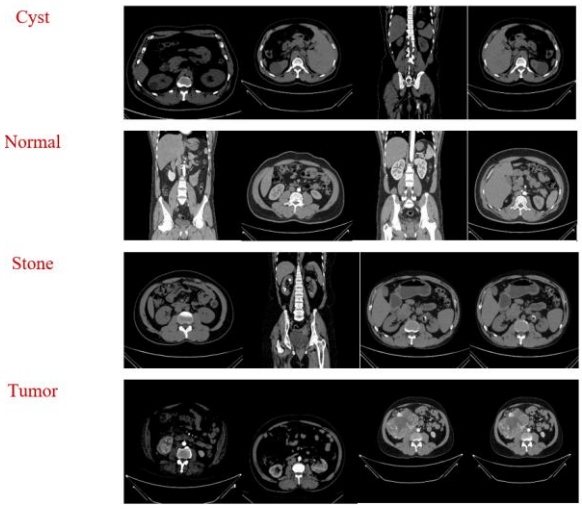

Fig. 3: Sample images of dataset

There are a total of 12,446 images in the collection, including coronal and axial cuts from contrast and non-contrast urograms and abdominal CT scans. Of these, 5077 are considered normal, 3,709 are cysts, 1,377 are stones, and 2,283 are tumours. A 512×512 pixel size was used for every CT scan. You can find the dataset on Kaggle, and Table 3 shows its class distribution.

This CT kidney dataset includes the pictures seen in Figure 1. We took ethical considerations into account in our experiment. Although no specific reference to ethical approvals or consent is included in the dataset description, it is widely believed that open-source datasets adhere to ethical standards. Patients are usually asked for their consent to use de-identified data when it is being collected. It is often the data provider's obligation to ensure compliance with privacy standards for datasets collected and shared on platforms such as Kaggle. Drawn from PACS in Dhaka, Bangladesh, the dataset comprises 12,446 images with class imbalance that is, 5077 normal against 1377 stone images. The research does not address explicit balancing or augmentation methods, even though the dataset is varied with coronal/axial views and contrast/non-contrast scans. To improve contrast, reduce noise, and standardise image quality before feature extraction and classification, however, considerable preprocessing was done utilising techniques including Gaussian Blur + Laplacian Filter (GB + LF), Median Blur + Laplacian (MB + LP), and Bilateral Filtering.

Enhancement of Image

There are a number of methods for improving images, and we've used a mix of filters for this:

GB + LF

After the image (GB) is smoothed to reduce noise, the Laplacian filter is applied to emphasise edges, thereby improving contrast for feature extraction. The sensitivity of the LF has been reduced by applying GB. To lessen the impact of features and noise, Gaussian blur can be used to blur the image. As a 2D function, Gaussian looks like this:

$$G(b,a) = \frac{1}{2\pi\rho^2} f^{\frac{-b^2+a^2}{2\rho^2}} \quad (1)$$

Where the mean is zero, and the standard deviation is one. In a Gaussian blur, the four parameters are as follows: Src for source, dst for destination, and ksize for kernel size. The standard deviation in the x-direction in the Gaussian kernel is represented by the double type variable sigmax. If you want to see how the intensity changes, you can use a linear filter like the Laplacian filter. Consequently, edge detection programs rely heavily on it (Borges et al., 2022). After smoothing, this filter is typically used to make the image less sensitive to noise. In this case, greyscale photographs are typically used for both the input and the output. A window value in a Laplacian filter interacts with the values of nearby pixels. Filter coefficients are the names given to these numbers. The output of this filter is equal to the product of the filter coefficients and the values of the related images. An image with sharp edges is the result.

An image's Laplacian ( ) *K_b, a* is defined as follows for any intensity $J(b,a)$:

$$K(b,a) = \frac{\delta^2 J}{\delta b^2} + \frac{\delta^2 J}{\delta a^2} \quad (2)$$

A *LoG* function with a standard deviation in two dimensions takes the following form:

$$log(b,a) = \frac{1}{\pi\rho^4}\left[1 - \frac{b^2+a^2}{2\rho^2}\right] f^{\frac{-b^2+a^2}{2\rho^2}} \quad (3)$$

MB + LP

Also, we've used median blur, which works better for low level noises like salt and pepper and speckle noise, among others. Using MB, the median of adjacent pixels is used to substitute individual pixel values. Because of this, we can get rid of pixels that don't add anything to the scene. This process is not linear. When trying to lessen the effect of salt and pepper noise, it is a popular choice. Eliminates salt and pepper noise via median filtering before Laplacian based edge improvement

Bilateral Filter

Considers spatial closeness and pixel intensity similarity to help preserve edges while lowering noise. By

simultaneously decreasing noise and smoothing the image, a bilateral filter maintains the image's edges. When blurring photos, a bilateral filter makes sure that only pixels with values close to the core pixels are taken into account. The intensity change and edges are both helped by this:

Linear Gaussian smoothing is the first step:

$$g(b) = (e * H^8)(b) = \int_{-Q}^{\cdot} e(a)H^8(b-a)da \quad (4)$$

This is where the distance $g(a) = H(b - a)$ determines the weight for $\|b - a\|$, which is equal to $g(b) - g(a)$. Additionally, this filter incorporates a weighting factor that is dependent on tone distance. At the end, it comes to:

$$g(b) = \frac{\int_{-Q}^{\cdot} e(a)H^8(b-a)H^s(g(b)-g(a))da}{\int_{-Q}^{\cdot} H^8(b-a)H^s(g(b)-g(a))da} \quad (5)$$

The three parameters that make up the bilateral filter are as follows: "d" for the diameter of the adjacent pixels, sigmaColor for the value in colour space, and "sigmaSpace" for the value in coordinate space.

Removal of Bony Skeleton

Many high intensity regions, including bed-mat, bones, vascular calcification, stones, and noise, remain in the images even after soft organs have been removed. The rib cage, vertebral column, and pelvic cage make up the bone skeleton, the greatest component among these undesirable sections (Thein et al., 2018). Also, kidney stones can enlarge to the size of a golf ball. The size of the skeletal skeleton differs significantly from the size of kidney stones. Also, locating the area of items in the image that is the largest can help remove it. We create this algorithm for the purpose of deleting bony skeletons:

- First step: Use the following equation to find the area of each three-dimensional item in the image:

$$Area\,(B) = Number\ of\ voxels\ in\ an\ object \quad (6)$$

- Find the greatest object area, P_{max}, in Step 2
- Third, divide the image into two sets of pixels, $h(w,z)_1$ and $h(w,z)_2$, and use P_{max} in the equation below to segment each set:

$$h(w,z) = \begin{cases} 1 & if P_{max} = h(w,z) \\ 0 & otherwise \end{cases} \quad (7)$$

- Fourth, create a new picture using $h(w,z)_2$ and ignoring $h(w,z)_1$

Removing Bed-Mat and Noise Reduction

The last step in kidney stone segmentation is to extract the bed-mat and any remaining noise from the image. To filter out undesirable items that are about the same size as stones, area based thresholding is not an option. In order to get rid of the bed mat, vascular calcification, and some noise that is left behind after the skeletal skeleton is removed, location-based thresholding was created. The *X*-, *Y*-, and *Z*-axis bed-mat is retrieved by use of a location-based thresholding technique. The bed-mat is precisely situated behind the bony skeleton, at the end of the Y-axis. In addition, kidney stones can develop in any part of the encased skeletal system the urinary tract, the kidneys, or the bladder. Based on the *X*, *Y*, and *Z* coordinates, the bed mat has been manually extracted from the image. Both the removal of bed mats and the lowering of noise (which is situated in front of the bone skeleton) are possible with the suggested location-based thresholding. The suggested solution isn't very robust, but it can eliminate bed mat noise entirely.

Feature Extraction-Second Order Statistics (GLCM)

The Gray-Level Co-occurrence Matrix (GLCM), which describes the spatial connection of pixel intensities, was used to create second-order elements (Munir and Imran, 2025). Gray-Level Co-occurrence Matrix (GLCM) was applied to extract second-order statistical variables, including contrast, correlation, energy, and homogeneity, thereby providing texture-based distinction indispensable in kidney stone identification. Especially for identifying density changes in stone areas, GLCM performs better than other methods, including HOG, SIFT, or wavelet transforms, in capturing textural nuances in greyscale CT images. It might, however, underperform in capturing global spatial patterns where CNNs or deep features are more successful. These features have been extracted:

- Contrast Determines the degree of colour difference between two pixels:

$$Contrast = \sum_{j,i}(j-i)^2 O(j,i) \quad (8)$$

- Correlation Shows that the intensity of each pixel is linearly dependent on one another:

$$Correlation = \frac{\sum_{j,i}(j.i.O(j,i)) - \tau_w \tau_z}{\rho_w \rho_z} \quad (9)$$

- Energy Stands for how consistently the intensity is distributed:

$$Energy = \sum_{j,i} O(j,i)^2 \quad (10)$$

- Homogeneity Measures how near the distribution is to the diagonal:

$$Homogeneity = \sum_{j,i} \frac{O(j,i)}{1+|j-i|} \quad (11)$$

Algorithm 1: Feature Extraction Algorithm for Plant Disease Dataset

Algorithm 1: Kidney Stone Detection Algorithm

Step 1
Input CT Images: Commence with a dataset of CT images featuring kidney stones.

Step 2
Image Resizing: Adjust the images to a uniform format appropriate for model processing, ensuring computational efficiency and consistency.

Step 3
Image Enhancement: It consists of three types: GB+LF, MB+LP, and BF

Step 4
Removal of Bony Skeleton

Step 5
Removal of Bed – Mat and Reduction of Noise

Step 6
Feature Extraction

Step 7
Identification of Kidney Stones: Employ the feature-extracted images to ascertain the presence and placement of kidney stones within the segmented regions.

Step 8
Dimensions & Specifications Detection: Ascertain the dimensions and pertinent characteristics of discovered kidney stones, extracting features essential for the ensuing classification task.

Step 9
Establish Hybrid ConvDBN Model: Configure a Hybrid ConvDBN model by setting parameters such as convolutional layers, learning rate, and batch size.

Step 10
Specify batch size, training iterations, convolutional layer design, and learning rate to enhance the model's training efficacy.

Step 11
Divide Data for Training and Testing (80: 20 Ratio): Partition the dataset into training and testing subsets, designating 80% for training and 20% for testing to evaluate the model's generalisation capacity.

Step 12
Execute Training Procedure: Train the Hybrid ConvDBN model on the training dataset, while evaluating training and validation accuracy throughout the process. Document the duration of the training.

Step 13
Conduct Testing Operation: Assess the trained model using the testing dataset, determining accuracy and supplementary metrics for an exhaustive performance evaluation.

Step 14
Comparative Analysis: Perform a comparative analysis of the accuracy and performance metrics between the proposed Hybrid ConvDBN model and traditional approaches. Emphasise any enhancements in detection accuracy and efficiency obtained by the suggested method.

Algorithm 1 involves preprocessing ultrasound images, training a Hybrid ConvDBN model, and evaluating its performance on the test dataset (Devi and Devi, 2024). The comparative analysis aims to demonstrate the efficacy of the proposed strategy for kidney stone diagnosis compared to conventional approaches.

ConvDBNTraining

Pretraining Algorithm for Sparse Penalty Mechanism for CRBM Model

Since the hidden layer is substantially bigger in dimension than the visible layer, the CRBM model is over-completing. Because they are not dependent on one another, convolution kernel parameters are learnt from training samples separately. When the training samples have comparable traits, it becomes easy for the CRBM's convolution kernels to become homogeneous due to the high degree of similarity in the learnt parameters. In the pre-training stage, a common method is to apply a sparse constraint that sets the majority of the hidden layer units to zero in order to reduce the activity of all the units.

A CBAM is used with the aim of achieving the sparse representation of RBM. The findings demonstrate that this approach outperforms the SP term based on the sum of squared errors in terms of learning effect. This study draws on this notion to integrate the CBAM term into the pre-training phase of CRB, specifically:

$$\Delta a_k^{sparisity} = o \log\left(\frac{1}{M}\sum_{m=1}^{M} r_l^m\right) + (1-o)\log\left(1-\frac{1}{M}\sum_{m=1}^{M} r_l^m\right) \quad (13)$$

In this context, $\Delta a_k^{sparisity}$ l denotes the l-th penalty term of bias, M stands for the batch size, o denotes the sparse coefficient, and r_l^m represents the mean activation probability value of the hidden layer output relevant to the l-th kernel convolution of the m-th sample, that is:

$$r_l^m = \frac{1}{M_G \times M_G}\sum_{j=1}^{M_G}\sum_{i=1}^{M} o\left(g_{ji}^l / U\right) \quad (14)$$

Whenever the CRBM parameters are modified, i.e:

$$\Delta a_k = \frac{1}{M_G \times M_G}\sum_{j,i}\left(g_{ji}^0 - g_{ji}^l\right) + \Delta a_k^{sparisity} \quad (15)$$

Complex DL problems can be handled using abstract features from automated learning, according to theoretical studies. This effect increases as the number of layers of deep learning increases (Hongmei and Pengzhong, 2021). Nevertheless, when the number of network layers increases, the gradient will vanish during backpropagation. To address the issue of the gradient fading during CDBN training, a solution that alternates between supervised and unsupervised training is presented. Figure 2 shows the training procedure of the CDBN network, which is detailed below:

- To finish the first layer of CRBM's (CRBM1) unsupervised learning, the pre-training algorithm is used

DOI: 10.3844/jcssp.2026.3042.3052

- By directly adding the classifier to CRBM1's pooling layer, we also introduce sample labels and utilise the BP technique to supervise parameter tuning of the network
- With the completion of the unsupervised learning for CRBM2, the output of the redesigned CRBM1 pooling layer is utilised as the input for CRBM2. The guided parameter correction procedure follows immediately after
- Carry on with steps (1) through (3) for all of the CRBM layers until you reach the very top of the network

It is possible to acquire the network's parameters after the training procedure. In the testing phase, the pictures are fed into the network, and the detection outcomes are extracted.

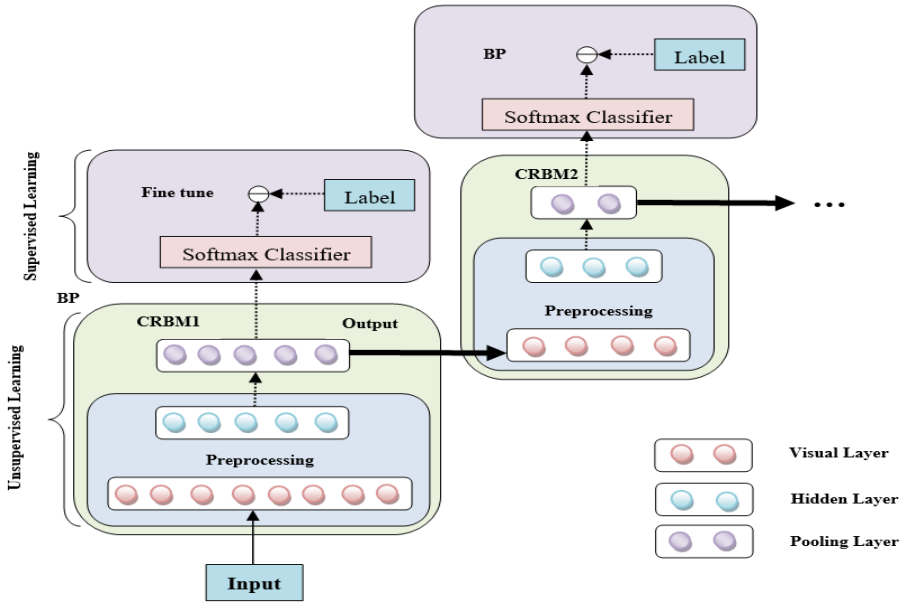

Fig. 2: Training process of ConvDBN

Results and Discussion

Kidney illnesses arise from multiple aetiologies, which can be broadly categorised into neoplastic and non-neoplastic conditions. NN applied to medical imaging is a recognised approach for advanced data mining and an emerging area of specialisation, enabling accurate management of renal illnesses. This review will present the fundamental methodology of imaging-based NN and its recent clinical applications in both neoplastic and non-neoplastic renal disorders. Furthermore, we examine its present obstacles and future potential, concluding that attaining data balance, resolving heterogeneity, and controlling data volume continue to pose difficulties for imaging based NN.

When evaluating the model's effectiveness, it is essential to analyse all of these metrics concurrently. Precision shows the percentage of correct kidney stone predictions, whereas recall shows how well the necessary positive predictions are made. The F1-Score is a harmonic mean of recall and precision. Using 175 test instances, the model's accuracy rate was 98.2%, and its sensitivity level was 96.66%. Table 2 summarises the performance metrics that were acquired using our suggested model and the testing data. Table 2 contrasts several models. The suggested ConvDBN exhibits higher precision (0.99), recall (0.97), and F1-score (0.98) than the other models. Particularly in cases of support (number of samples) rather high (n = 175 for kidney stone class), these values show statistically significant improvements. Though statistical testing e.g., t-tests, confidence intervals is absent, the performance differences between CNN-KNN and DBN are sufficient to claim superiority.

Here we may see histograms of the model's first-order features. Features like these, culled from the dataset, show you the whole range of possible values for each feature. Every histogram shows the distribution of frequencies for a particular characteristic; the x-axis shows the values of the features, and the y-axis shows how often each value appears. Figure 3 displays the histogram of the following variables: GLCM contrast, correlation, energy, and homogeneity.

The training and validation performance data, including the F1 score, are displayed graphically in Figure 4 over epochs. The validation epochs with the best validation accuracy and lowest validation loss are

DOI: 10.3844/jcssp.2026.3042.3052

highlighted. Convolutional layers followed by Restricted Boltzmann Machines with a sparse penalty mechanism form the ConvDBN. Deeper than simple CNNs, it avoids the complexity of residual connections (ResNet) or encoder-decoder designs (U-Net). Although the work lacks specific FLOPs or runtime analysis, it suggests reasonable computing cost with better accuracy. Although the alternating supervised-unsupervised training of the hybrid model raises training complexity, it improves convergence and resilience.

Table 2 shows that the percentages for the models trained using our suggested training technique outperform those for the models trained independently. Once again, when trained separately, ConvDBN outperformed all other models on evaluation metrics. As with the suggested training approach, other independently trained models also exhibit the same performance order in terms of quantitative performance. Additionally, the training and validation losses of each trained model were used to validate it.

Figure 5 shows that every cell represents two classes, one actual and one expected. The intensity of colour in each cell represents occurrence frequency. Intense colouration along the heatmap's diagonal highlights the model's accuracy in picture classification. The model's performance across all classes is concisely and insightfully summarised in this graphic depiction.

The loss function was a combination of the Dice and cross-entropy. Validation loss was used to pick the top models after training. For each model, Figure 6 displays the training loss and validation loss. The paper does not specifically say if external test sets or k-fold cross-validation was used. Rather, to assess generalisation, a train-test split technique dividing data into training and testing subsets was used. This reduces the claim of robustness; so, the study would gain from cross-validation or external dataset evaluation to increase dependability.

Table 2: Comparison of models

Models	Precision	Recall	F1-Score	Support
Kidney Stone	0.99	0.97	0.98	175
Normal	0.97	0.99	0.98	172
Accuracy			0.98	347
Macro Avg	0.98	0.98	0.98	347
Weighted Avg	0.98	0.98	0.98	347

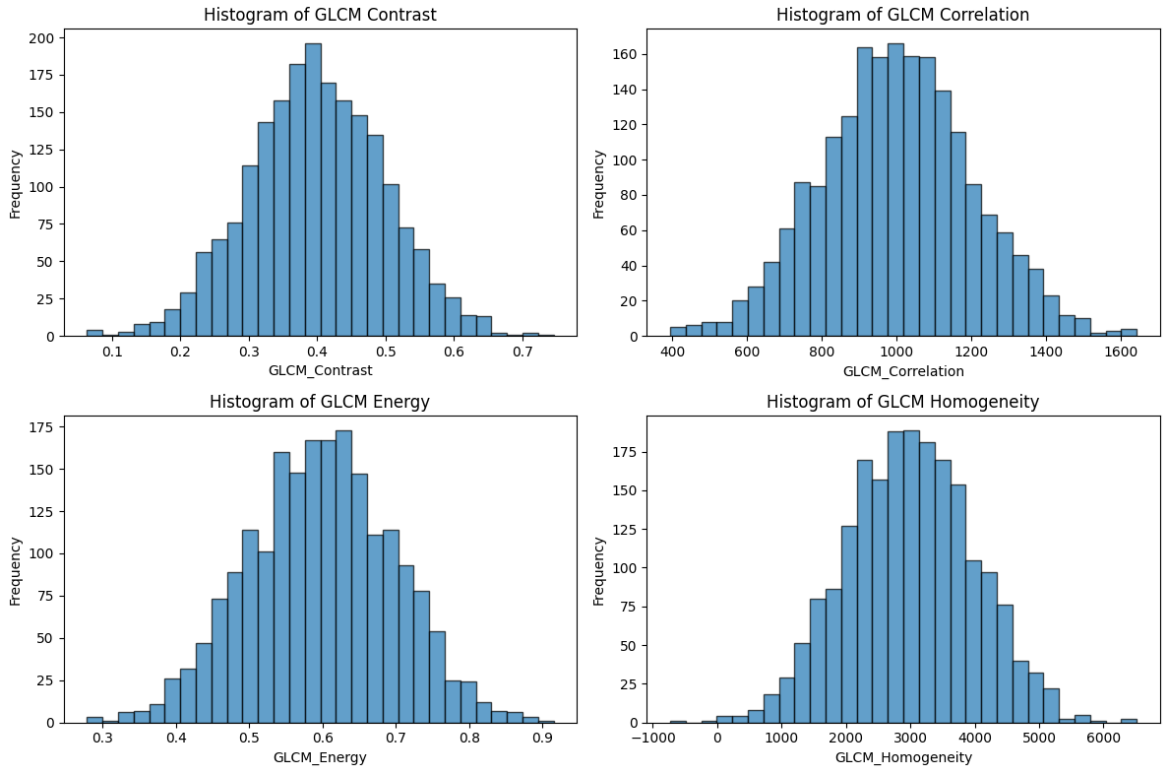

Fig. 3: Histogram of second order GLCM feature

DOI: 10.3844/jcssp.2026.3042.3052

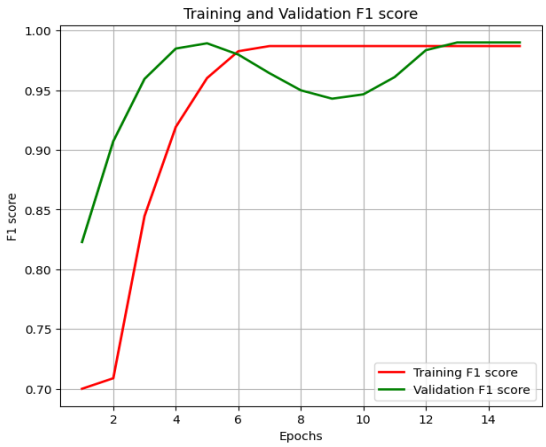

Fig. 4: F1 score value of the proposed model

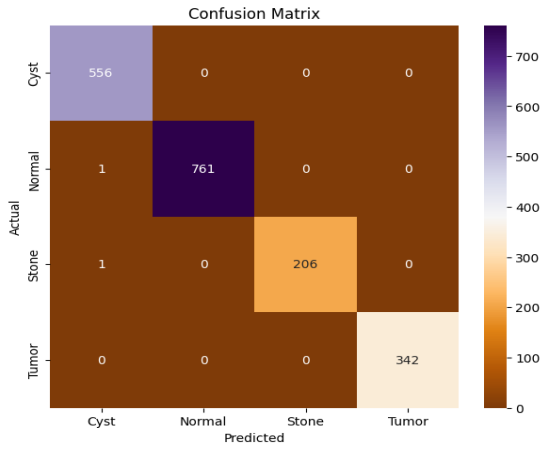

Fig. 5: Proposed model confusion matrix

A graph showing the relationship between classification error and the number of characteristics used is shown in Figure 7. The picture shows a correlation between feature count and classification error rate as a function of feature percentage. On one side, we have the number of characteristics (x-axis), which can take on values between 0 and 200, and on the other, we have the classification error (y-axis), which can take on values between about 0.01 and 0.03. There is no discernible pattern to the rising or falling trend in the shown classification error with increasing feature counts. The green line indicates that classification error varies greatly depending on the features chosen, and the variations further support this idea. Figure 7 shows changing categorisation error with feature count. The non-monotonic pattern suggests that some features could cause noise or redundancy, so not all elements equally support accuracy. The green line indicates error fluctuation, therefore verifying the need for feature selection and the identification of optimal subsets to reduce classification error.

Figure 8 is a bar graph that contrasts these several evaluation indicators. Though the model is suggested for clinical decision support, real-world implementation or usability testing with radiologists or clinicians is not included.

Though lacking validation in a clinical environment or human-in-the-loop feedback to demonstrate interpretability, workflow integration, or practical benefits, the system is theoretically solid and demonstrates outstanding accuracy (98.2%). When compared to competing models, ConvDBN always comes out on top across all four measures. CNN-KNN trails behind, indicating it is a formidable competitor.

Table 3: Different preprocessing techniques for GIN classification

Models	Kidney Stone	Normal	Specificity	Sensitivity	Accuracy
CNN	80.7	93.2	89.5	74.8	88.5
DBN	74.4	66.8	93.1	90.3	92.4
CNN-SVM	42.23	60.4	90.9	70.5	90.6
CNN-KNN	78.7	93.8	95.7	94.2	95.3
KNN	60.54	72.8	89.8	79.2	89.7
ConvDBN	95.2	96.2	98.5	97.5	98.2

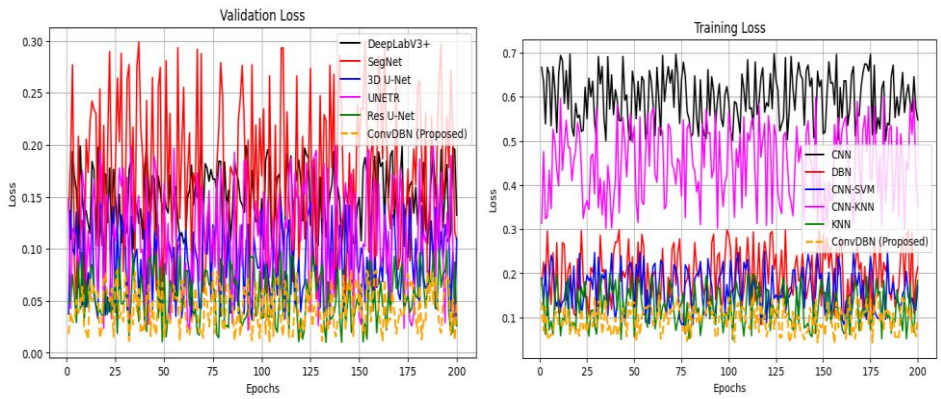

Fig. 6: Validation and training loss of the models

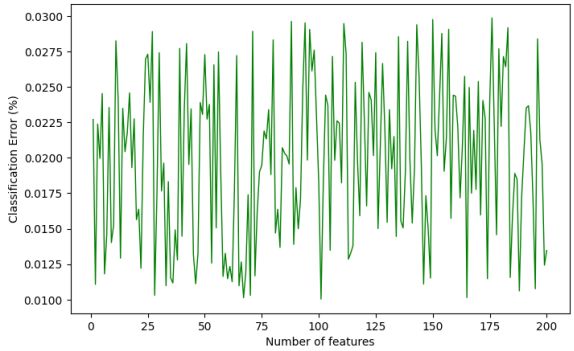

Fig. 7: Classification error for the proposed model

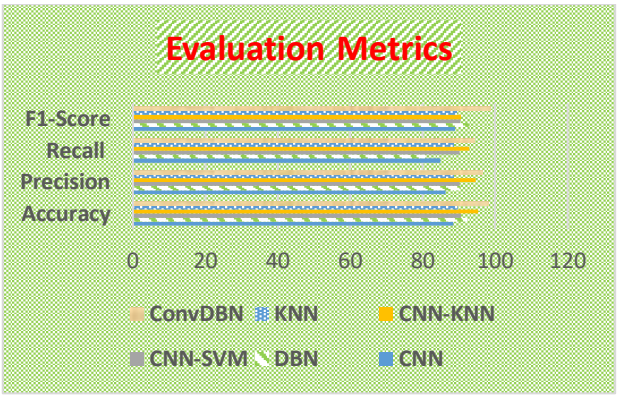

Fig. 8: Different evaluation metrics

The performance of KNN and CNN is moderate when compared to hybrid models. When compared to CNN-KNN, DBN shows competitive performance but is marginally less effective. Although it falls short of optimal performance, CNN-SVM maintains consistency.

Conclusion

This research presents an automated method for kidney stone diagnosis utilising CT scan images and advanced neural network algorithms. This study aims to identify and categorise various kidney ailments, including stones and normal structures. Our project aims to revolutionise the diagnostic process by providing an accurate and efficient automated system for kidney stone assessment utilising the robustness of the ConvDBN architecture. The methodology incorporates a meticulously curated dataset encompassing diverse kidney disorders, facilitating comprehensive model training, validation, and evaluation. The model employed augmentation techniques and preprocessing methods tailored for medical imaging data to enhance its ability to recognise intricate patterns and characteristics associated with different kidney disorders. The model exhibited exceptional accuracy in classification, yielding promising results in identifying and distinguishing distinct kidney disorders. The model exhibited exceptional precision in differentiating between stones and normal structures, and it displayed robustness in complex medical imaging scenarios. This study provides a comprehensive overview of our methodology, dataset preparation, preprocessing, model design, and detailed performance analysis. We evaluate the merits and drawbacks of our methodology and provide avenues for future enhancement. This research enhances medical image analysis, paving the way for improved precision medicine and superior healthcare diagnostics.

Acknowledgment

The authors would like to appreciate the effort of the editors and reviewers.

Funding Information

This research received no specific grant from any funding agency in the public, commercial, or not- for-profit sectors.

Author's Contributions

All authors contributed equally.

Ethics

There are no human subjects in this article, and informed consent is not applicable.

Conflict of Interests

The authors declare that they have no conflicts of interest.

References

Ahmed, F., Abbas, S., Athar, A., Shahzad, T., Khan, W. A., Alharbi, M., Khan, M. A., & Ahmed, A. (2024). Identification of kidney stones in KUB X-ray images using VGG16 empowered with explainable artificial intelligence. In *Scientific Reports* (Vol. 14, Issue 1, p. 6173). https://doi.org/10.1038/s41598-024-56478-4

Aksakalli, I., Kacdioglu, S., & Hanay, Y. S. (2021). Kidney X-ray Images Classification using Machine Learning and Deep Learning Methods. In *Balkan Journal of Electrical and Computer Engineering* (Vol. 9, Issue 2, pp. 144–151). https://doi.org/10.17694/bajece.878116

Almuayqil, S. N., Abd El-Ghany, S., Abd El-Aziz, A. A., & Elmogy, M. (2024). KidneyNet: A Novel CNN-Based Technique for the Automated Diagnosis of Chronic Kidney Diseases from CT Scans. In *Electronics* (Vol. 13, Issue 24, p. 4981). https://doi.org/10.3390/electronics13244981

Asif, S., Zheng, X., & Zhu, Y. (2024). An optimized fusion of deep learning models for kidney stone detection from CT images. *Journal of King Saud University - Computer and Information Sciences*, *36*(7), 102130. https://doi.org/10.1016/j.jksuci.2024.102130

Bayram, A. F., Gurkan, C., Budak, A., & Karataş, H. (2022). A Detection and Prediction Model Based on Deep Learning Assisted by Explainable Artificial Intelligence for Kidney Diseases. In *European Journal of Science and Technology* (Vol. 40, pp. 67–74). https://doi.org/10.31590/ejosat.1171777

Borges, T., Rai, A., Raj, D., Ather, D., & Gupta, K. (2022). Kidney Stone Detection using Ultrasound Images. In *SSRN Electronic Journal* (pp. 1–8). https://doi.org/10.2139/ssrn.4159208

Busi, R. A. L., Meka, J. S., & Reddy, P. V. G. D. P. (2023). A Review: Analyzing Risk Factors and Prediction for Chronic Kidney Disease using Machine and Deep Learning Techniques. In *2023 2nd International Conference on Automation, Computing and Renewable Systems (ICACRS)* (pp. 1456–1462). https://doi.org/10.1109/icacrs58579.2023.10404903

Devi, J. S. S. C., & Devi, D. S. C. (2024). A Hybrid Model for Kidney Stone Detection Using Deep Learning. *Internation Journal of Science Technology and Management*.

Hongmei, W., & Pengzhong, L. (2021). Image recognition based on improved convolutional deep belief network model. In *Multimedia Tools and Applications* (Vol. 80, Issue 2, pp. 2031–2045). https://doi.org/10.1007/s11042-019-08300-x

Huang, J., Hou, J., Yang, W., Zhan, M., Xie, S., Li, S., Li, R., Wu, S., He, Y., Zhao, W., Zhang, R., Shan, G., & Ni, W. (2023). Automatic Kidney Stone Composition Analysis Method Based on Dual-energy CT. In *Current Medical Imaging Formerly Current Medical Imaging Reviews* (Vol. 20, p. e080923220827). https://doi.org/10.2174/1573405620666230908111745

Kazemi, Y., & Mirroshandel, S. A. (2018). A novel method for predicting kidney stone type using ensemble learning. *Artificial Intelligence in Medicine*, *84*, 117–126. https://doi.org/10.1016/j.artmed.2017.12.001

Kidney Dieses Detection (normal-cyst-tumor-stone. (n.d.). *Kaggle*.

Kumar, D., Chandar, K. P., Malik, N., Balasubramanian, K., Suganthi, D., & Babu, G. C. (2024). Enhanced Detection of Kidney Stones using Level Set Segmentation and Kernel-ELM. *2024 International Conference on Data Science and Network Security (ICDSNS)*, 1–6. https://doi.org/10.1109/icdsns62112.2024.10690917

Lopez-Tiro, F., Estrade, V., Hubert, J., Flores-Araiza, D., Gonzalez-Mendoza, M., Ochoa, G., & Daul, C. (2024). On the In Vivo Recognition of Kidney Stones Using Machine Learning. *IEEE Access*, *12*, 10736–10759. https://doi.org/10.1109/access.2024.3351178

Ma, L., Qiao, Y., Wang, R., Chen, H., Liu, G., Xiao, H., & Dai, R. (2024). Machine Learning Models Decoding the Association Between Urinary Stone Diseases and Metabolic Urinary Profiles. *Metabolites*, *14*(12), 674. https://doi.org/10.3390/metabo14120674

Manjunatha, D., Vishwakarma, V., Mishra, A., Ravindran, E., & Kumari, K. B. M. (2024). Kidney Stone Detection Using Ultrasonographic Images by Support Vector Machine Classification. *Nanotechnology Perceptions*, *20*(S2), 93–106. https://doi.org/10.62441/nano-ntp.v20is2.8

Munir, S., & Imran, M. (2025). Detection of Kidney Stones using CT Scan Imaging. *ResearchGate*, *13*(8), 24–343.

Nedbal, C., Adithya, S., Naik, N., Gite, S., Juliebø-Jones, P., & Somani, B. K. (2024). Can Machine Learning Correctly Predict Outcomes of Flexible Ureteroscopy with Laser Lithotripsy for Kidney Stone Disease? Results from a Large Endourology University Centre. *European Urology Open Science*, *64*, 30–37. https://doi.org/10.1016/j.euros.2024.05.004

Pande, S. D., & Agarwal, R. (2024). Multi-Class Kidney Abnormalities Detecting Novel System Through Computed Tomography. *IEEE Access*, *12*, 21147–21155. https://doi.org/10.1109/access.2024.3351181

Rajan, P. G., Sapra, P., Mary, S. S. C., Chauhan, A., Parte, S. A., & Nishant, N. (2023). Hybrid Convolutional Neural Network and Extreme Learning Machine for Kidney Stone Detection. *2023 Second International Conference on Electronics and Renewable Systems (ICEARS)*, 936–942. https://doi.org/10.1109/icears56392.2023.10085243

Ramesh, P. S., Patel, S., Bamane, K. D., UshaRani, Y., Tiwari, M., & Karthikeyan, T. (2023). Automatic Kidney Stone Detection Using Deep learning Method. *Journal of Advanced Zoology*, *44*(S4), 100–109. https://doi.org/10.17762/jaz.v44is4.2176

Thein, N., Nugroho, H. A., Adji, T. B., & Hamamoto, K. (2018). An image preprocessing method for kidney stone segmentation in CT scan images. *2018 International Conference on Computer Engineering, Network and Intelligent Multimedia (CENIM)*, 147–150. https://doi.org/10.1109/cenim.2018.8710933

Zhang, M., Ye, Z., Yuan, E., Lv, X., Zhang, Y., Tan, Y., Xia, C., Tang, J., Huang, J., & Li, Z. (2024). Imaging-based deep learning in kidney diseases: recent progress and future prospects. *Insights into Imaging*, *15*, 50. https://doi.org/10.1186/s13244-024-01636-5

Zhu, G., Li, C., Guo, Y., Sun, L., Jin, T., Wang, Z., Li, S., & Zhou, F. (2024). Predicting stone composition via machine-learning models trained on intra-operative endoscopic digital images. *BMC Urology*, *24*(1), 5. https://doi.org/10.1186/s12894-023-01396-2